SENSITIVITY ANALYSIS OF SEISMIC ATTRIBUTES PARAMETRIZATION TO REDUCE MISINTERPRETATIONS: APPLICATIONS TO DEEPWATER CHANNEL COMPLEXES

Authors —Karelia La Marca*[1], Heather Bedle[1], Lisa Stright[2], and Kurt Marfurt[1]

[1] School of Geosciences, The University of Oklahoma, 100 East Boyd St. Suite 710 Norman, OK 73019. [2] Department of Geosciences, Colorado State University, 322 Natural Resources Building, Fort Collins, CO 80523-1482.

Email: karelialm@ou.edu, hbedle@ou.edu, lisa.stright@colostate.edu, kmarfurt@ou.edu

Original paper date of submission: February 2023

Revised paper date of submission:

ABSTRACT

Geoscientists apply algorithms such as seismic attributes to better interpret depositional systems that enhance various aspects of the seismic data. However, they are limited by the original seismic amplitude or frequency content, data quality, and algorithm parameters considered.

Additionally, our capacity to interpret depositional system architecture is limited by seismic resolution, which results in potential misinterpretations associated with the correct position of stratigraphic features. This is particularly important as mapping reservoir architecture (geobody size, shape, and stacking patterns) in the subsurface is critical for exploring and producing hydrocarbons, CO_2 storage, and geothermal resource development since it can define connectivity or compartmentalization of flow zones.

To address these concerns, we investigated five synthetic seismic volumes from low to high-frequency bandwidths of 15 Hz, 30 Hz, 60 Hz, 90 Hz, and 180 Hz based on an architectural model of an outcropping deepwater channelized slope system in the Magallanes Basin, Chile. We analyzed 1) how seismic bandwidth affects the resolution of stacked stratigraphic features (i.e., deepwater channel elements and Mass Transport Deposits (MTDs)) and their subsequent seismic interpretation, and 2) the effect of different seismic attributes commonly employed in channel interpretation on our data to understand the "mixing" or "vertical smearing" of stratigraphic features by comparing the seismic with the true geological model 3) we explored how the attributes' parametrization affects the imaging of differently sized features by modifying the analysis window in each case from +/-2ms to +/- 50 ms. Finally, 4) we evaluated the effect of different noise levels in the sensitivity analysis.

Results show that the "mixing" of events occurs mainly as a result of 1) the seismic bandwidth, 2) the algorithm used for each seismic attribute calculation, 3) the attribute vertical analysis window, and 4) the signal-to-noise ratio of the data. Broadband, higher frequency data, and small analysis windows provide clearer images of the stacked channels. In contrast, low-frequency data and larger analysis windows result in more mixing or "composite" appearances, affecting interpretations and net-to-gross estimates, especially in small-size stratigraphic features such as individual channel elements and Mass Transport Deposits (MTDs). Our observations warn of potential misinterpretations in applying default attributes to actual seismic data, especially in geometrical attributes and window-dependent ones. Recognizing these misinterpretations is paramount for reconstructing deepwater architecture (this study), sedimentary and structural studies for drilling locations, reserves estimation, and overall uncertainty assessment.

Keywords: deepwater; seismic facies; architectural elements; seismic geomorphology; interpretation; seismic attributes; channel complex, analysis window.

1. Motivation and objectives

Seismic exploration of deepwater channels is challenging due to the physical properties inherent to the seismic, the variability in fill and stacking of reservoir geobodies, and the uncertainty that can occur due to the lack of hard data (core or well data). Reservoir architecture controls the distribution of fluids in the subsurface and the connectivity (or compartmentalization) of the reservoir that impacts recovery or injectivity. Therefore, geoscientists seek to understand how sensitive the interpretation of reservoir architecture is to different quality and types of seismic data, as well as different attributes and parameters commonly used to identify the architecture better and to make appropriate well plan decisions, volumetric and recovery/storage estimates.

The primary questions we aimed to address with the study are:

- How does the seismic data's frequency content affect the imaging of deepwater architecture?
- What is the effect of each seismic attribute on the architecture interpretation and its true position, both vertically and horizontally?
- What is the effect of the seismic attribute analysis window size on the vertical smearing of architecture?
- What is the effect of seismic noise on our sensitivity analysis?

The study's importance is identifying common pitfalls in seismic interpretation using synthetic seismic data created from an outcrop-derived architectural model of a seismic-scale deepwater channel system. Studies with synthetic data like this allow geoscientists to understand uncertainty in interpreting channel architecture from seismic data.

2. Introduction

When it comes to reservoir characterization using seismic reflection data, even if we employ all the tools available to interpret, locate, and measure the reservoir that will contain (oil, gas, and water) or allow for the storage (geothermal, CO_2) of economic resources, uncertainty prevails. This interpretational ambiguity occurs due to changes in various physical parameters in response to the media and the seismic records' inherent acquisition and processing characteristics.

The imaging and interpretation of different-sized stratigraphic features in the subsurface using seismic reflection data are often compromised due to limits in seismic resolution, which in addition to tuning effects, can influence volumetric interpretations and gross rock volume calculations (Pemberton et al., 2018). Therefore, geoscientists need to understand the common pitfalls associated with seismic interpretation: the impact of the frequency content on the imaging of reservoir architecture, the choice of parameters and attributes' influence on the interpretation of architectural elements, and the detrimental impact noise can have on the overall picture. To address this, we performed a sensitivity analysis that evaluated four parameters: frequency content, the effect of the seismic attribute, the impact of the window of analysis, and noise level combined with five 3D synthetic datasets.

The synthetic data that was derived from an outcrop analog in Magallanes Basin, Chile (Ruetten, 2021), and employed realistic acoustic impedances. The models that used a series of zero-phase Ormsby wavelets and 1D convolution (Langenkamp et al., 2021) allowed us to better understand how seismic bandwidth and seismic attribute parametrizations affect the resolution of stacked stratigraphic features in a seismic-scale channel system, providing insights that could be beneficial to the industry for drilling decisions, whether it is for hydrocarbon, geothermal, or CO_2 storage purposes.

In order to extract the most value and information from the seismic data, seismic interpreters often derive seismic attributes from the data to reveal additional stratigraphic or structural features. These attributes provide a means to enhance vertical and lateral changes in reflectivity, thickness, continuity, and orientation of seismic features. From the exhaustive list of seismic attributes existent, we focus on amplitude-derived, instantaneous, and geometric attributes for offering promising results in channel architecture definition (La Marca, 2020). All coherence algorithms (that belong to the geometric attributes' class) use a vertical and lateral analysis window, whether they are based on cross-correlation, semblance/variance, eigenstructure analysis, or the gradient structure tensor. For good quality data, Marfurt et al. (1998) found it best to analyze stratigraphic features using a temporal analysis window as narrow as possible, determined by the highest frequency in the data or the 3rd frequency corner in the

Ormsby wavelets. For poor-quality data, a larger window approximating the dominant period of the data provides improved results with minimal stratigraphic mixing.

Pemberton et al. (2018) and Langenkamp (2021) provided insights into the effect of amplitude and frequency on architectural element imaging and interpretation and facies classification. Nonetheless, the impact of seismic attributes, the parameters, and the noise content were not evaluated. Hence, this is one-of-a-kind study that focuses on assessing the complexities of attribute parameterization using synthetic data based on a known geologic model.

With the true model known, attribute parameterization and its effects on stratigraphic interpretation can be quantified, particularly highlighting the parameters that impact the apparent stratigraphic mixing or smearing of events such as the windows of analysis.

We first describe the aspects related to the architectural (outcrop) model and the characteristics of the synthetic datasets used. Then, our workflow is explained, providing details on the four parameters evaluated. Results are presented and focused on the cases derived from parameter combinations/sensitivity analysis. In the end, we provide a table and workflow that allows geoscientists to identify potential pitfalls in interpretation and address them according to their individual datasets, as best practices in interpretation should be documented and available to the geoscientific community to help reduce uncertainty in reservoir characterization.

3. Geological model description

The geological model that is the basis of this study is derived from a sandstone-rich deepwater channel system along a progradational slope system (Hubbard et al., 2010). These deepwater slope deposits from the Late Cretaceous (70-80 Mya) Tres Pasos Formation are exposed on approximately 3 km long, 200m thick outcrops near Laguna Figueroa in the

Magallanes Basin, Southern Chile (Macauley and Hubbard, 2013; and Hubbard et al., 2014). The high quality of the stacked channel systems has been used to construct a seismic-scale 3D architectural model of the deepwater channel system (Pemberton et al., 2018; Jackson et al., 2019; Langenkamp et al., 2020; Ruetten, 2021). According to Fildani et al. (2013) the outcrop is analogous to many slope channel systems globally in stratigraphy and depositional setting, which makes it an excellent benchmark for any study that aims to address problems associated with channel interpretation.

The models are the result of several studies from Macauley and Hubbard (2013), Fletcher (2013), and Southern et al. (2017) combining measured sections, hierarchical stratigraphic interpretations, paleoflow measurements and thousands of GPS data points that calibrated a drone-derived photomosaic. For these models, the fundamental architectural component are channel elements, defined as distinct, mappable channelized sedimentary bodies (Figure 1). Multiple stacked, related channel elements form a channel complex, and two or more complexes form a channel complex set (McHargue et al., 2011; Macauley and Hubbard, 2013, Meirovitz et al., 2020; Figure 1). The outcrops at Laguna Figueroa contain two complex sets, simply referred to as the Upper and Lower Figueroa. The upper complex set consists of eight channel elements and are grouped into four distinct channel complexes. The lower complex set contains twelve channel elements grouped into three channel complexes. Elements are modeled with a standardized width of 400 m and thickness of 25 m. Three additional architectural components are present in the outcrop: mudstone drapes at the base of channel elements, mass transport deposits (MTDs) at the base of channel complexes, and inner-levee thin-bed deposits encasing the channelized elements (Macauley and Hubbard, 2013; Hubbard et al., 2014). The geological models consist of five facies: 1) channel element axis in yellow, 2) channel element off-axis in orange, 3) channel element margin in brown, 4) homogeneous shale in gray, and 5) background shale (inner and outer levee facies) in white (Figure 2C).

Jackson et al. (2019) developed the first fine-scale geocellular model combining channel planforms and vertical stacking for the lower outcrop section (lower channel system) but did not include hierarchical groupings in the architecture. Pemberton et al., (2018) generated forward seismic models using Jackson et al. (2018)'s model and analyzed seismic interpretation of architecture as a function of seismic resolution. Nielson (2018) analyzed the tuning effects of single channel elements. Ruetten (2021) updated Jackson's initial model with new interpretations and added an upper channel system separated from the lower system by a debris flow, and studied how stacking patterns impact reservoir connectivity and fluid flow. Finally, Langenkamp (2021) analyzed the influence of stacked channel element architecture on facies classification using Ruetten's model. This work utilizes the geocellular model of Ruetten (2021) and synthetic seismic models from Langenkamp (2021).

The five synthetic seismic models used in this study were built using a series of zero-phase Ormsby wavelets of 15 Hz, 30 Hz, 60 Hz, 90 Hz, and 180 Hz and 1D convolution (Chile Slope Systems research consortium; Langenkamp et al., 202; Figure 2C) with a reflectivity model. More aspects of each model are found in Langenkamp (2021). Facies-based rock properties (Figure 2B), adopted from Stright et al. (2014), show that amplitude peaks represent an increase in acoustic impedance (Figure 2D). In contrast, troughs depict a decrease in acoustic impedance. The synthetic volumes have a vertical window of 500 ms. For analysis purposes, we cropped the volume from 120ms to 380ms to avoid dead/blank zones in the reflectivity and focus on the target channel systems.

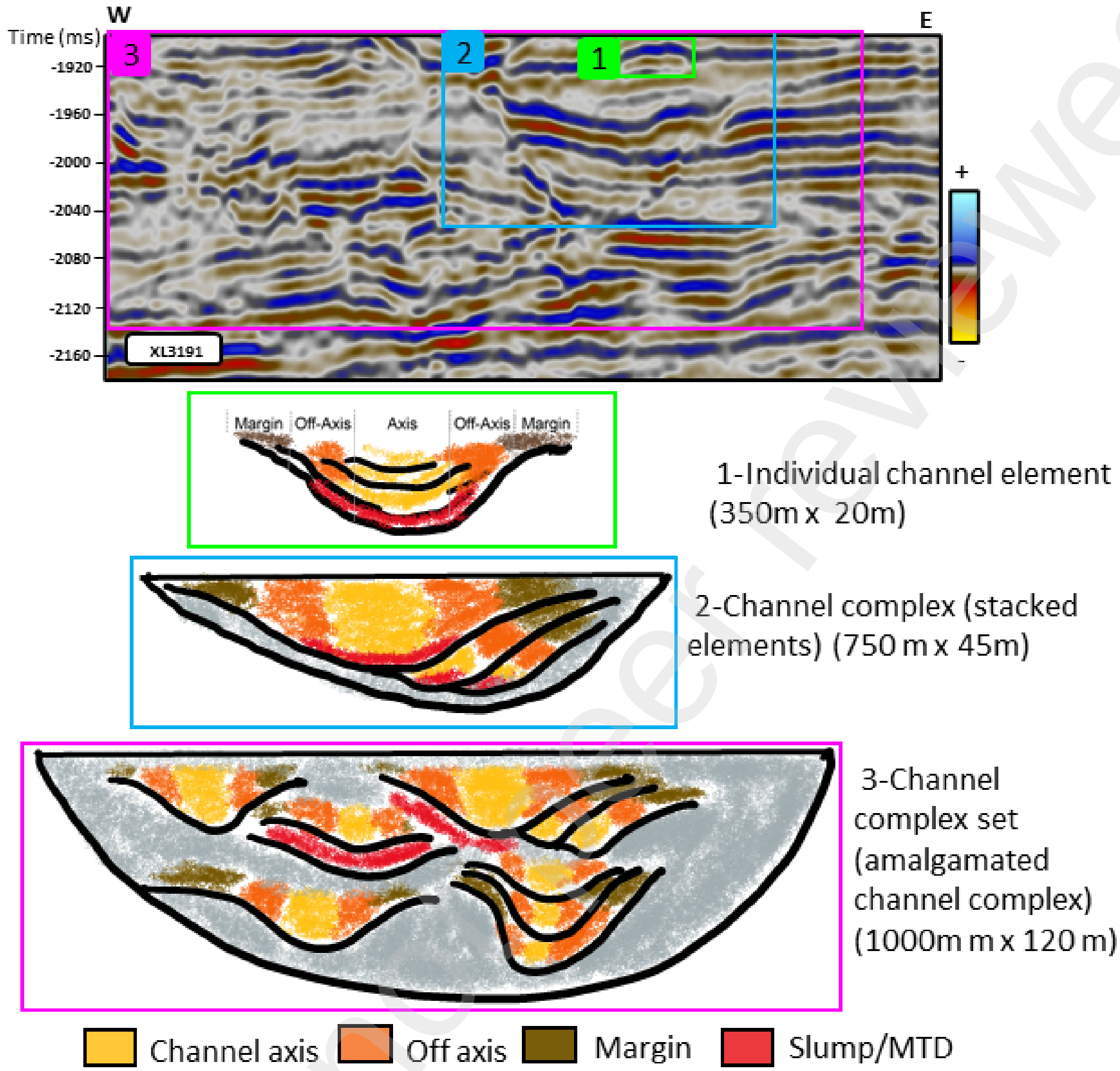

Figure 1. Stratigraphic hierarchy: from a single element to complex sets. A vertical slice within the Pipeline 3D dataset offshore New Zealand shows the seismic appearance of different architectural hierarchies in deepwater channels, with corresponding cartoons below. The smallest architecture (4th to 5th order) is the channel element (box 1 in green). The second hierarchy (6th order) occurs when the channel elements stack together, forming a channel complex (box 2 in blue). The higher-order hierarchy (7th order and higher) occurs with the amalgamation of channel complexes, developing a channel complex set (box 3 in magenta). The color legend indicates the distinct facies that commonly occur within each element of each architecture. Measuring the sizes of each architectural element indicated on the right as well as their hierarchy, provides key insight into the underlying depositional processes as well as a prediction of the more common lithologies. Hierarchies mentioned follow Pickering and Cantalejo (2015) classification.

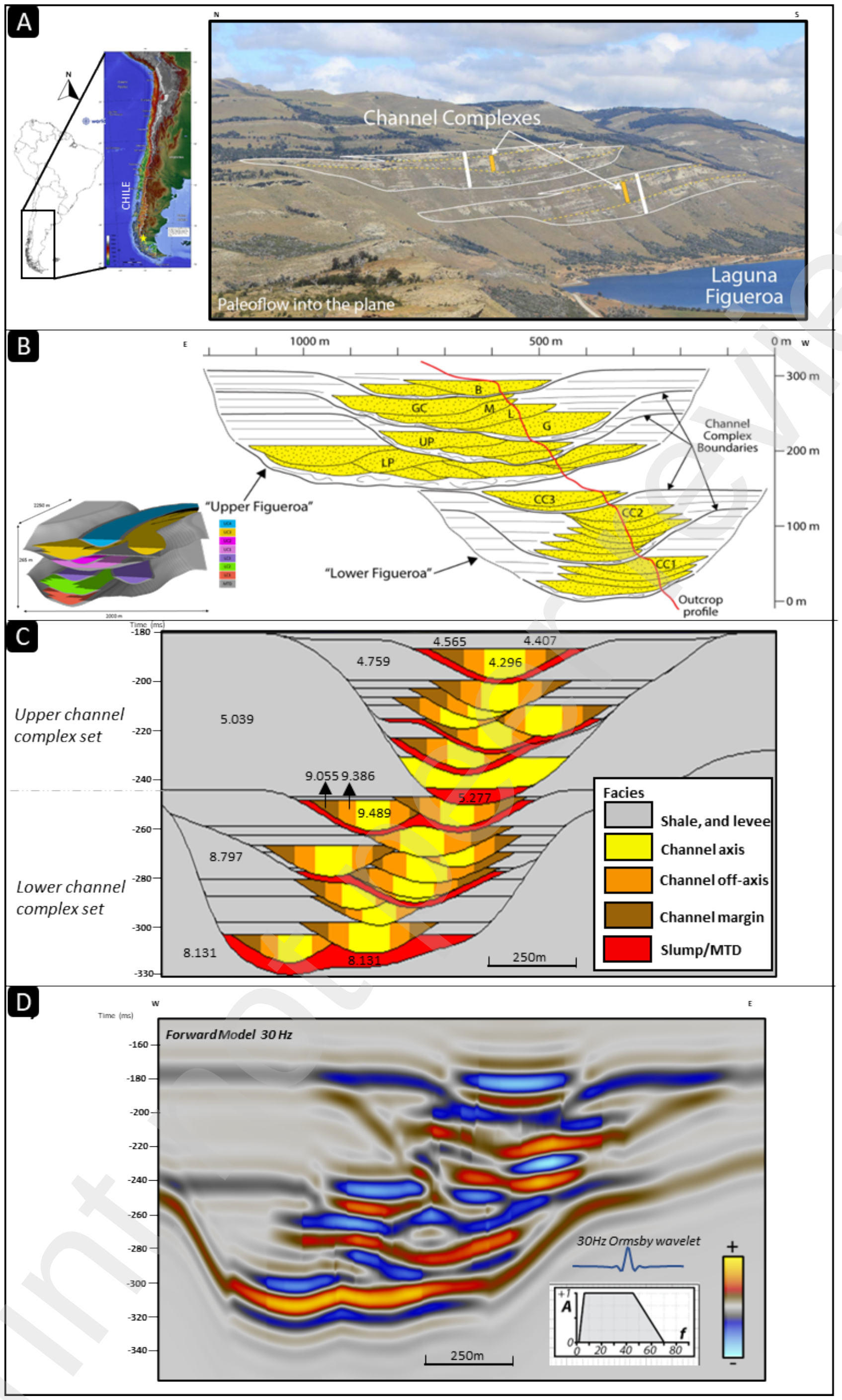

Figure 2: A visual guide showing the steps to convert outcrop measurements to a synthetic model. (A) Location and exposure of the outcropping deepwater channels at Laguna Figueroa. Paleoflow is from North to South (obliquely and to the right into the outcrop at this location) (B) Conceptual diagram of the Upper and Lower Figueroa outcrops showing channel elements, complexes, and complex sets. The red line indicates the outcrop profile. Left of the line is into the outcrop face, and the right has been eroded away. (C) geocellular model using the constraints from (B) augmented by facies and corresponding rock properties, including acoustic impedances from Shallow Offshore West African modeled rock properties (Stright et al., 2014). (D) The Ormsby wavelet and a representative vertical slice through the 3D synthetic seismic data volume generated from the model shown in (C). Courtesy of Teresa Langenkamp and Lisa Stright.

4. Methods

To address the questions posed in the study and focus on analyzing the effect of bandwidth on vertical resolution, we introduce the term "stratigraphic event mixing." This vertical smearing phenomenon is explained in Figure 3, using a real example where the interference of channels from other stratigraphic levels is evident. As depicted in Figure 4, first, we performed an exploratory data analysis to define a vertical window of interest constrained to the objective of the study: 120 ms and 380 ms from our five volumes of synthetic seismic data. After cropping the 15 Hz, 30 Hz, 60 Hz, 90 Hz, and 180 Hz dominant frequency volumes, we performed a sensitivity analysis on four parameters: 1) frequency content, 2) seismic attribute effect, 3) the effect of the analysis window, and 4) the influence of band-limited random noise.

Next, we calculated a series of seismic attributes from amplitude accentuating, geometric, and instantaneous attributes commonly employed in seismic interpretation of channel systems. Due to the number of cases to evaluate, we decided to explore and present the most representative seismic attributes for each case in detail (the most commonly used and that provided better results). Next, for each scenario, we defined a suite of 3-trace by 3-trace analysis windows with various vertical lengths from 2 ms to 50 ms. For visualization and interpretation purposes, we used co-rendering techniques. Finally, we explored the impact of the addition of low and high levels of noise.

The final analysis of the results was performed by combining the aforementioned parameters into the following cases: 1) the response on the same attribute and analysis window in the different bandwidth volumes, 2) the impact of changing the analysis window for different seismic attributes, 3) the effect of changing the window of analysis size for the same seismic attribute, and 4) the effect of noise. All cases were contrasted with the initial actual data/model.

More details and considerations taken in each parameter evaluation are presented below.

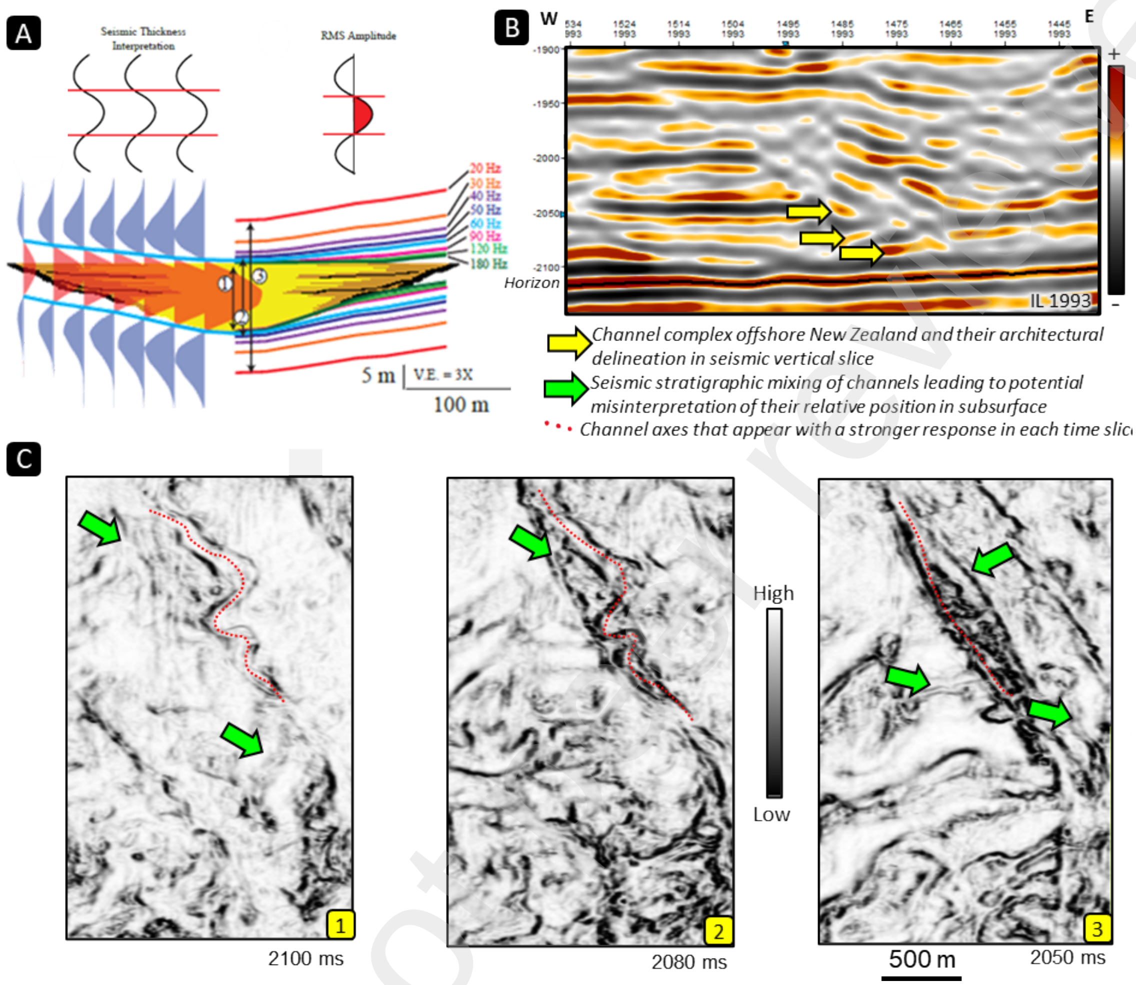

Figure 3. Explanation of stratigraphic event mixing or vertical smearing of stratigraphic features. (A) Vertical resolution of channel elements related to different peak frequencies (modified after Nielson, 2011). (B) Vertical slice through the 3D Pipeline 3D offshore New Zealand seismic survey showing a channel complex and a Horizon used for interpretation at different stratigraphic levels indicated by yellow arrows. The dominant frequency at this level is 40 Hz giving a dominant period of 25 ms. (C) Stratal slices at approximately 25 ms intervals through the coherence volume computed using a ±20 ms analysis window show "stratigraphic" mixing by the seismic wavelet. Note that the relatively straight channel form at 2050 ms can be seen at 2080 ms and other stratigraphic levels (1,2,3 from deeper to shallower) where other channel forms (green arrow) appear causing interference. The cause of this mixing could be 1) mixing of reflectivity by the 25ms dominant period seismic wavelet, 2) mixing of discontinuities through the 40 ms coherence computation, 3) shifting of the basal channel element thalweg due to compensational style as you move up or 4) differential compaction over deeper discontinuities between the floodplain and the channel element fill.

4.1. Parameter 1: frequency content effect

Tuning thickness is the temporal resolving power of seismic data. Some authors use resolution and tuning thickness terms interchangeably, although tuning starts right below the vertical resolution. Table 1 presents the tuning thickness for each element in the synthetic volumes studied here. Knowing the resolvability in seismic is paramount to understanding the effect of other parameters considered in the sensitivity analysis.

Resolution is the ability to resolve by seismic interpretation methods two features that are close together. By definition, the vertical resolution of seismic data is ¼ of the wavelength (λ), where the λ is determined by dividing the average velocity by the dominant frequency.

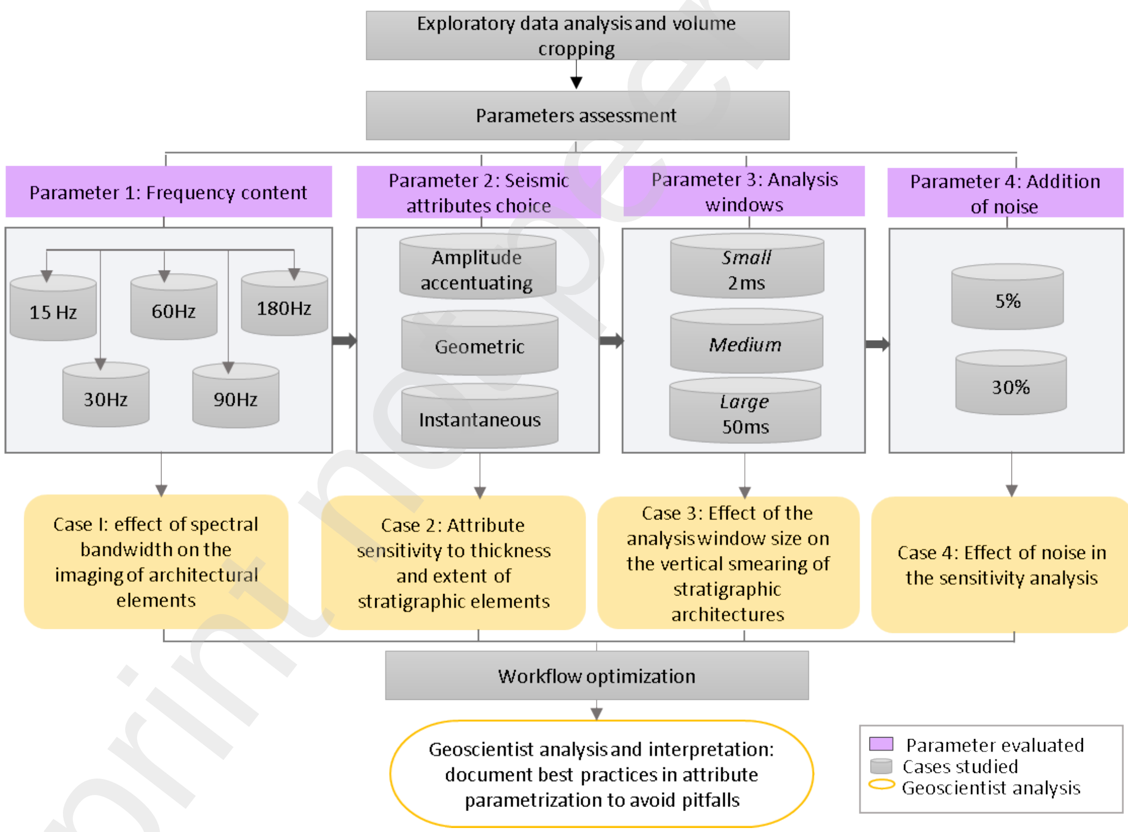

Figure 4. Workflow of the study. Four different parameters were evaluated in the sensitivity analysis: 1) the effect of frequency content, 2) the impact on the choice of the seismic attribute, 3) the analysis window effect, and 4) the sensitivity to band-limited random noise addition. The best cases were selected to be shown in each case, and analysis was performed by comparing them with the original 3D geological model derived from the Laguna Figueroa Deepwater outcrop. This resulted in 4 cases for analysis, ultimately leading to a workflow and documentation of best practices in channel architecture interpretation.

The frequency content was the first parameter evaluated for the impact on the interpretation and resolvability of the different architectural elements. The five dominant frequency synthetic seismic volumes were analyzed, and we compared the results with those of Pemberton et al. (2018), and Langenkamp (2021).

	Channel elements	**MTDs**
Dominant Frequency (Hz)	**Tuning Thickness (m)**	**Tuning Thickness (m)**
15	48.9	53.2
30	24.4	26.6
60	12.2	13.3
90	8.1	8.9
180	4.1	4.4

Table 1. Tuning thicknesses for shallow and deep elements in each synthetic seismic volume. Modified from Langenkamp (2021).

4.2. Parameter 2: Choice of seismic attributes

A seismic attribute is a computation made from algorithms applied to seismic data to get a more interpretable output. These responses relate to rock physical properties (La Marca, 2020) in rocks and fluids in the subsurface. However, there are tens if not hundreds of seismic attributes (Barnes, 2016), and time constraints do not allow for testing them all. Some of the latest studies (Posamentier and Kolla, 2003; Chopra and Marfurt, 2007; Hossain, 2020; and La Marca and Bedle, 2022) have proven the successful application of amplitude accentuating, geometrical and instantaneous attributes applied to PSTM data to interpret and characterize channel elements and complexes in both fluvial and deepwater settings. Generally, we need the combination of a geometrical attribute that allows defining edges and at least one attribute that provides insights into stratigraphy (La Marca et al., 2019) to characterize channel features in seismic data. Therefore, we focused on testing attributes that belonged to those three attribute categories and chose the most prominent of each class.

Table 2 summarizes the most representative seismic attributes selected for each class: root mean square amplitude (RMS), Sobel filter coherency, and instantaneous frequency.

Attribute	Appearance	Attribute Category	Measurement	Use in architecture interpretation
Coherence	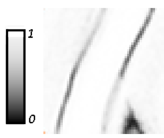	Geometric	Direct measure of waveform similarity or how similar waveforms or traces are in a volume- used to emphasize continuous events or edges.	Delineates edges of channel elements
RMS amplitude	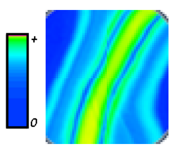	Amplitude/Energy	Measures the square root of the average energy within a vertical window.	Provides measure of channel element vs inner levee Provides statistical measures of channel element fill between two picked horizons
Instantaneous frequency	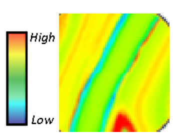	Spectral	A simple approximation of the mean frequency of the seismic wavelet.	Channel element thickness

Table 2. Selected seismic attributes to perform the sensitivity analysis showing a representative image, feature measurement, and use in channel element interpretation.

4.2.1. RMS amplitude

The RMS amplitude is an amplitude accentuating attribute often used for stratigraphic and lithologic variations enhancement. It is defined by the standard deviation, $\sigma(t)$, of the data, $d(t)$, within a running analysis window, subsequently measuring the reflectivity within that window (Meek, 2015). For a window that ranges from $-T=-K\Delta t$ to $+T=+K\Delta t$ about a sample j, the RMS amplitude is:

$$d_{RMS}(j\Delta t) = \sigma(j\Delta t) = \left(\frac{1}{2K+1}\sum_{K=K}^{+K}\{d[(j+k)\Delta t)]\}^2\right)^{1/2} \quad . \text{Eq (1)}$$

In this study, we evaluated how well RMS showed stratigraphic variations.

4.2.2. Coherence (Sobel Filter)

Seismic coherency is a measure of how similar traces are among their neighbors, which is a response to lateral changes in the seismic record caused by variations in structure, stratigraphy, lithology, porosity, and the presence of hydrocarbons (Marfurt et al., 1998), and it is determined computing amplitude derivatives along structural dip. Sobel filter (Luo et al., 1996) is one of the many coherence methods, which for seismic data normalizes coherence data to produce results between 0 and 1, where 0 is the lowest coherence, and 1 is the highest coherence. It has proven to be effective in delineating channel element edges (La Marca and Bedle, 2021; Hossain, 2020; and Herron, 2011); therefore, we aimed to test the definition of the channel elements' edges.

4.2.3. Instantaneous frequency

The instantaneous frequency is computed sample by sample, is the time derivative of the instantaneous phase $\varphi(t)$:

$$F(t)=\mathrm{d}[\varphi(t)]/\mathrm{d}t. \qquad \text{Eq (2)}$$

and provides a simple estimate of the mean frequency of an isolated seismic event.

Subrahmanyam and Rao (2008) find that the instantaneous frequency attribute can indicate bed thickness and provide lithology insights. Chopra and Marfurt (2007) emphasize their usefulness in identifying abnormal attenuation and thin-bed tuning. Our model has thin features, such as channel elements (from axis, off-axis, to margins), that we aimed to test by using this instantaneous attribute.

4.3. Parameter 3: Analysis window effect

According to Lin et al. (2014), the scale of the window height, H, is a function of the dominant or peak frequency f_{peak}:

$$H = 1/(2f_{peak}) \quad . \quad \text{Eq (3)}$$

Applying this concept to our dataset spectrum, we would need to use a window of 2ms for the highest frequency volume (180Hz) and ~33 ms for the lower frequency volume (15Hz).

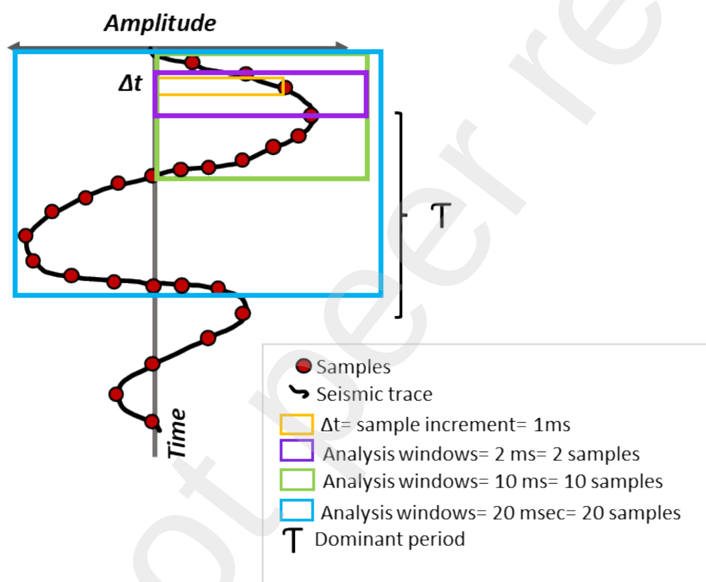

Figure 5. A representative analysis window used in attribute calculations. Signals are sampled at discrete points, not continuous recordings. Therefore, each seismic trace will contain as many samples as the sample rate allows. For the example shown, if we consider the dominant period (distance between two peaks), our analysis window will contain 20 samples, equivalent to ~ 20 msec. Other examples of analysis windows are depicted, including the smallest possible equivalent to the sample increment, in this case, 1 msec.

To understand the concept of analysis window, we have drawn a cartoon (Figure 5) that shows a seismic trace with its respective samples. It illustrates how a small, medium or large analysis window would look and what a dominant period is. Usually, the number of samples considered in a default analysis window parameter setting is around 11 samples (default window 60ms) for a 6ms sample rate dataset; in our dataset, the sample rate is 1ms. In real data, shallower, higher frequency data often shows smaller periods than the deeper strata/intervals where lobes of the traces are wider. Due to this change in frequency, some authors, like Lin et al. (2014), recommend using an adaptive window. However, this is not often possible or available in the software packages commonly used by geoscientists. Nonetheless, the geoscientist/interpreter can control the analysis window in the attribute settings. Therefore, we want to provide insights into the difference between a default analysis window and a shorter or larger one (which reduces or increases the number of samples, respectively). We compared the results from each different analysis window to the original, true data (the geological model), which provides a good sensitivity analysis for all kinds of datasets and any of the attribute families studied here.

4.4. Parameter 4: Addition of band-limited random noise

When seismic data is recorded, we find two components: signal and noise. The latter comprises all the unwanted recorded energy that contaminates seismic data, and it can be random or coherent (Kumar and Ahmed, 2021). Random noise is generated by activities in the environment where seismic acquisition work is being carried out, and this noise appears in a seismic record as spikes (Enwenode, 2014). Seismic noise levels depend on the type of acquisition—land or marine—and the intrinsic conditions unique to every site, such as climate, the burial of sensor, and wind (Tanimoto et al., 2015). Although there are many types of noise, like Gaussian, Pink, Brownian, violet, and blue, in this study, our fourth parameter incorporated in the sensitivity analysis is the band-limited random noise.

Signal-to-noise ratio (SNR) is a measure used to compare the degree of signal to the level of background noise, in which case a ratio larger than 1:1 suggests more signal than noise. So, the lower the SNR, the noisier our dataset. As Chen et al. (2019) mentioned, this will lower the quality of the seismic, affecting subsequent analyses such as imaging and inversion.

We incorporated different noise levels, from a low noise added of 5% to a high 30%. Higher noise levels were not presented due to the incapacity to extract meaningful interpretations from the data. Nowadays, noise can be added to synthetic datasets thanks to available software like the one used in this study.

5. Results

To address the study questions and link the parameters taken into account in the sensitivity analysis, we present the results summarized in four cases:

5.1. Case 1: The effect of the spectral bandwidth on the imaging of architectural elements

After evaluating the five synthetic models of 15 Hz, 30 Hz, 60 Hz, 90 Hz, and 180 Hz dominant frequencies, we observed that the level of detail of the different sized architectural elements increases with frequency; therefore, broadband, higher frequency provides better resolution.

Figure 6 shows the effect of each frequency in imaging each geological element. Figure 6B corresponds to the lowest frequency, and we can distinguish channel complexes and mass transport deposits (MTDs). However, smaller features like the 25m thick channel elements and MTDs are mixed in thicker, unresolvable reflectors.

Figures 6C and 6D show frequencies commonly encountered in the subsurface (30Hz and 60Hz for vintage and recent data, respectively). Here, the individual complexes are well-defined. Nonetheless, the amalgamation or stacking of elements presents a single response and minimal acoustic impedance contrast.

Higher frequencies shown in Figures 6E and 6F present the best responses compared to the original model. Figure 6E can even differentiate some of the stacked packages; overall, the individual and stacked channel elements can be better resolved. It is noteworthy how the highest frequency (180 Hz) illustrated in Figure 6F starts to lose the definition of the inner reflectors. Another observation is that, in all cases, the vertical channel axis (center) is resolved better than the channel's margins, both as a function of thickness (channel elements are thickest in the center at the axis) and acoustic impedance contrast (rock properties of channel element margin is more similar to inner levee than the channel element axis).

In general, channel complexes sets are visible at all frequencies analyzed, whereas individual complexes start to be resolvable from 30 Hz and higher. However, when elements have vertical stacking, channels do not show contrast in acoustic impedance due to repeated material/ similar composition and properties, therefore the attribute response is also affected by this phenomenon.

5.2. Case 2: Attribute sensitivity to thickness and extent of stratigraphic elements

After performing the seismic attribute sensitivity analysis, we noticed that the thickness and extent of stratigraphic events imaging are inherently linked to the frequency content of the seismic, analysis window, and seismic attribute used. At peak frequencies commonly encountered in the subsurface (around 30- 60Hz), the number of complexes was underestimated, and the size, shape, and type of architectural bodies (channels elements vs. margins, elements vs. complexes) were difficult to differentiate (Figure 7).

In most cases, channel complex sets were able to be interpreted. However, the amalgamation of smaller-scale channel elements results in an incorrect estimation of thicknesses. Nielson (2016) documented the same phenomenon.

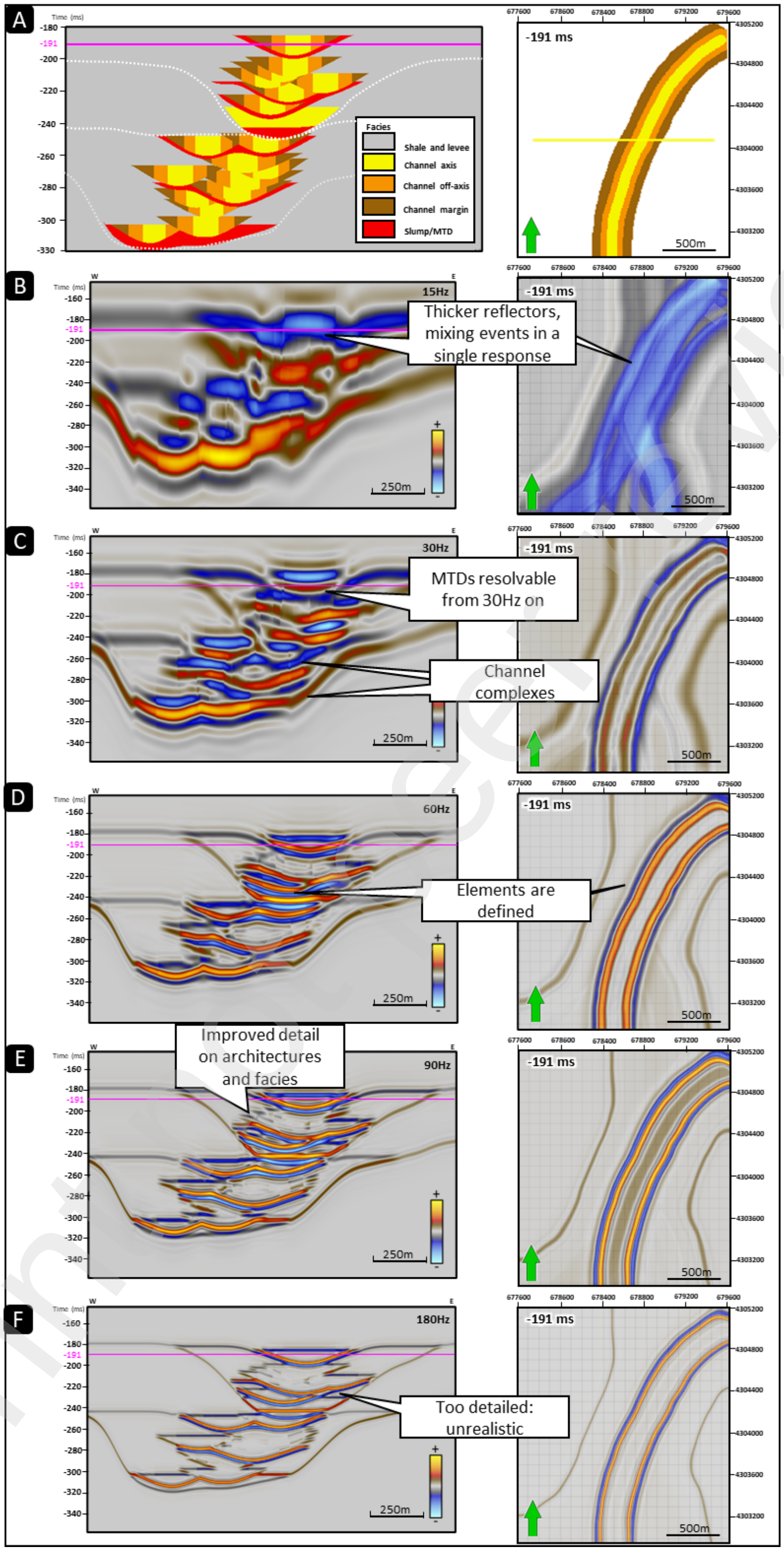

393

394 **Figure 6**. A representative vertical slice (224) and time slices at t=-191ms) through the (A) 3D model that
395 shows (B) 15 Hz data, (C) 60 Hz data, (D) 90 Hz data, and (E) 180 Hz data. Notice the improvement in the
396 channel architecture's detail with the increase in the dominant frequency and corresponding spectral
397 bandwidth, being able to interpret complexes from figure B on.

For example, in cases where similar facies were in contact, the acoustic impedance similarities did not allow for the differentiation of individual channel elements. Also, in tests performed with a large analysis window, the interpretation of smaller features was not possible (Figure 8B, 8D).

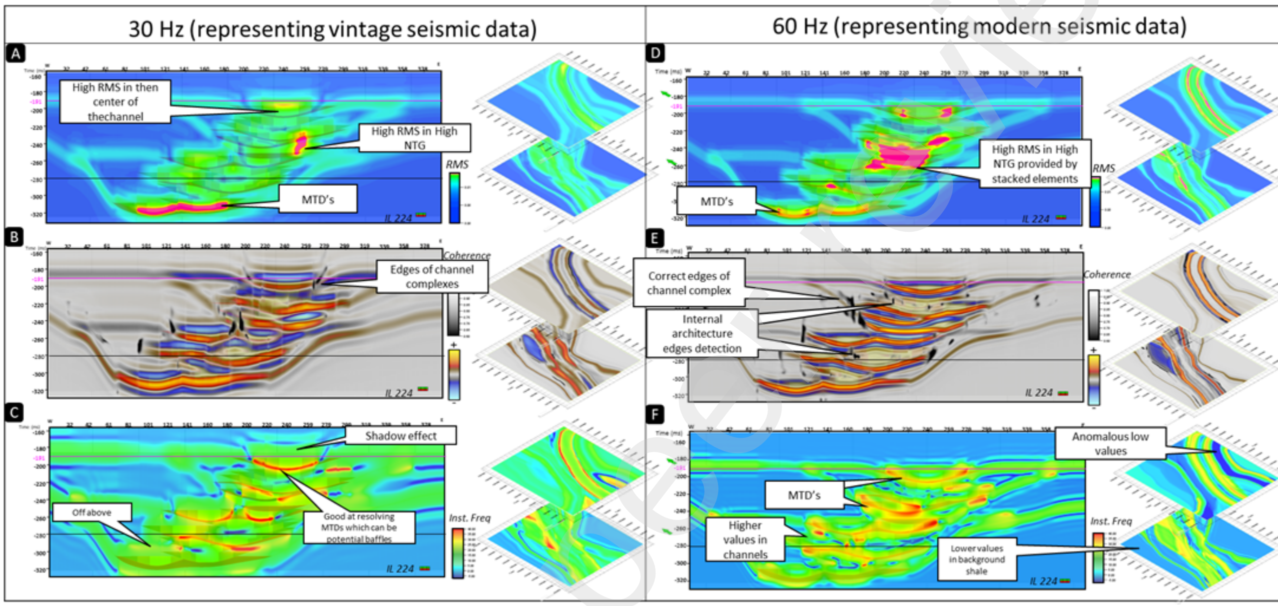

Figure 7. Results on the attribute sensitivity analysis to thickness and extent of architectural elements using a default analysis window. We present results on the 30 Hz dataset, analogous to vintage seismic data (to the left), and the 60Hz dataset, representing modern seismic data (to the right). Each attribute is presented for both frequencies in a representative inline (224) and time slices (-280 ms and –191ms) as follows: (A) RMS (Root Mean Square) amplitude for 30 Hz (B) coherence (Sobel filter) for 30Hz, (C) Instantaneous frequency for 30 Hz, (D) RMS amplitude for 60 Hz (E) coherence (Sobel filter) for 60Hz, (F) Instantaneous frequency for 60 Hz.

5.3. Case 3: Effect of the analysis window size on the vertical smearing of stratigraphic architecture

To demonstrate the effect of the window size on the vertical smearing of the different architectural elements in the model, we show an RMS amplitude sensitivity analysis (Figure 8). We perceived that RMS amplitude offers a detailed picture of the various facies in the 180 Hz volume, including imaging of the MTD associated with the channel complexes and the individual channel elements. However, for larger analysis windows and lower frequency volumes, for example, 50 ms window combined with a 15Hz dominant period seismic volume, such details are lost, resulting in an accentuated vertical stratigraphic smearing effect. Therefore, the application of amplitude-derived seismic attributes results more effective in higher frequency content datasets and using a small analysis window than in another configuration. It is noteworthy that a higher value of RMS is presented where an amalgamation of events occurs, which potentially leads to the interpretation of higher NTG (Figures 7 and 8).

Since the Sobel filter coherence seismic attribute aids in detecting discontinuities, such as geological structures and edges, especially in time slices, we included this attribute in our analysis to identify the channel complexes and the edges of the channel elements (Figure 9).

We observe stratigraphic mixing occurring in the vertical slices when we utilize a larger analysis window. It is also noticeable that higher dominant frequency data in combination with a small analysis window allows for a correct placing of feature edges (Figure 9C), which is supported when compared to the true model. In contrast, the position of the channel element edges deviates from the original/ true location or becomes distorted when the analysis window size increases (Figure 9D) or the frequency of the data is small (Figure 9A) regardless of the analysis windows used.

5.4. Case 4: Effect of noise in the sensitivity analysis

Figure 10 shows the most prominent results of the sensitivity analysis on the noise effect. We compared, in this case, how instantaneous frequency, coherence, and RMS amplitude seismic attributes respond to variations in band-limited random noise from 5% to 30%.

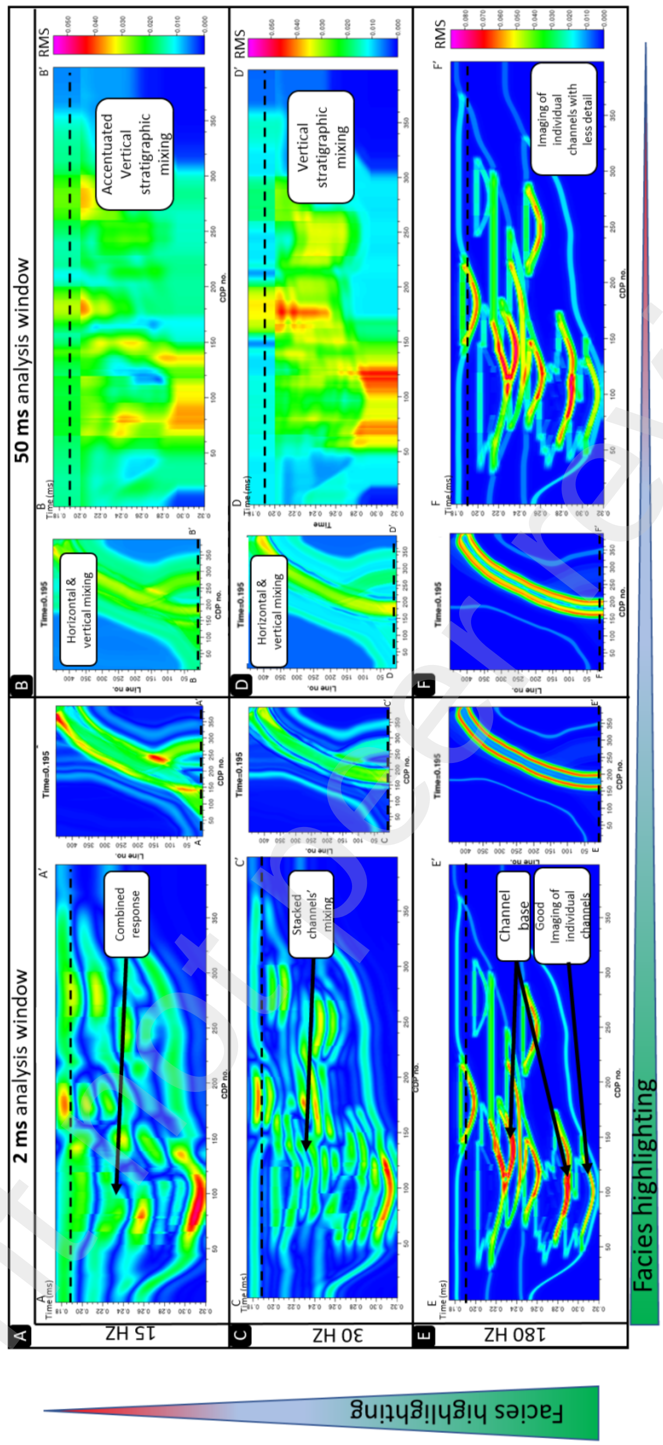

Figure 8. RMS amplitude sensitivity analysis to evaluate the effect of the window size *W* on the vertical smearing of the different channel elements in the model. (A) 15 Hz with *W*=2ms (B)50 Hz with *W*=50ms (C) 30Hz with *W*=2ms (D) 50 Hz with *W*=50ms (E) 180 Hz with *W*=2 ms (F) 180 Hz with *W*=50 ms. High-frequency data with a small analysis window provides the most suitable representation of the true model. In RMS amplitude, the most accurate facies depiction is given by high frequencies and small window combination, imaging channel element base, and inner and outer levee facies.

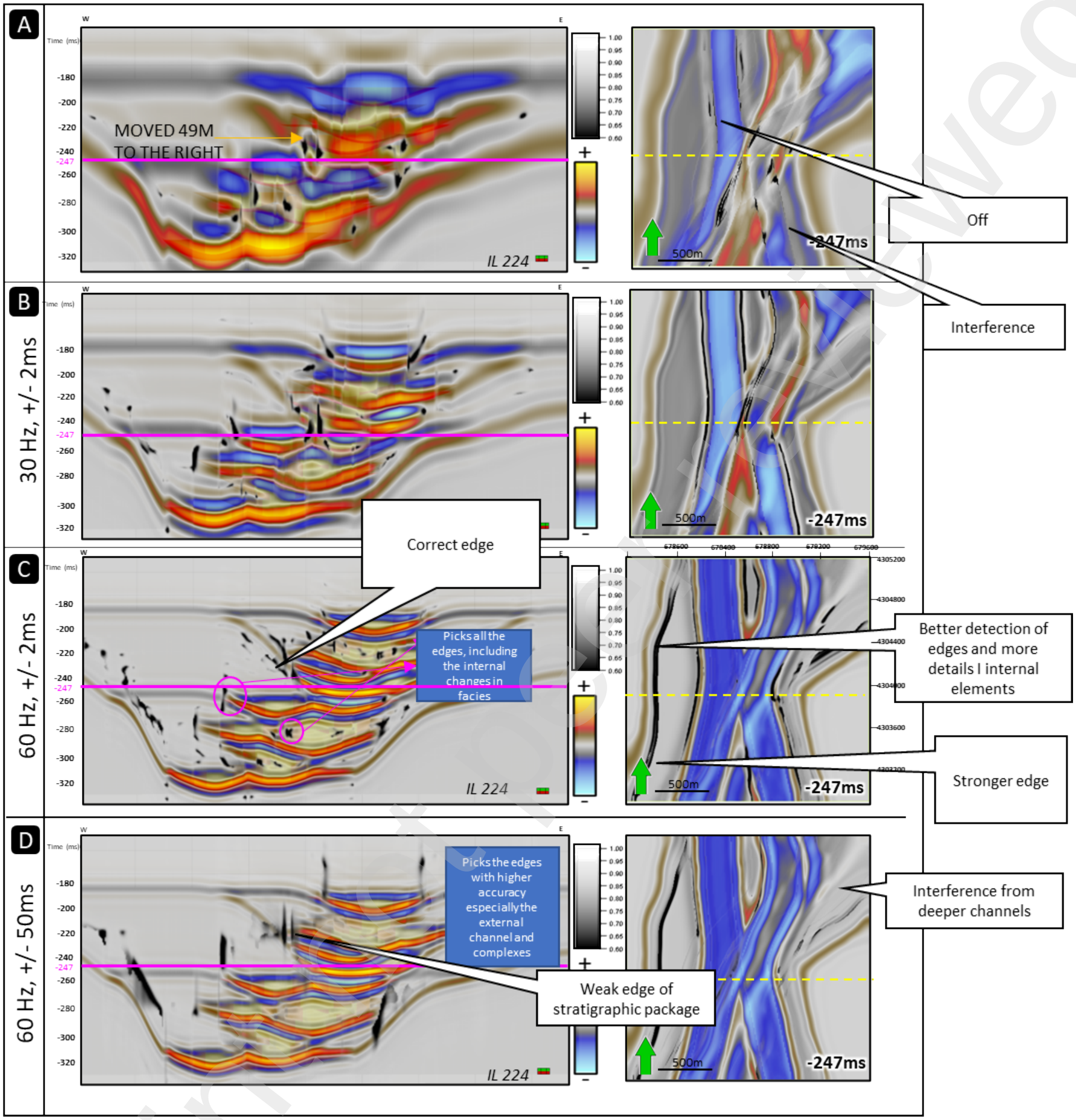

Figure 9. Sobel filter coherence attribute sensitivity analysis to evaluate the effect of the window size *W* on the vertical smearing and displacement of the different architectural elements in the model. (A) 15 Hz with *W*=2ms (B)30 Hz with *W*=2ms (C) 60Hz with *W*=2ms (D) 60 Hz with *W*=50ms. Notice how at a higher dominant frequency (60Hz) and smaller window of analysis, there is better detection of the channel element edges and channel element fill. In contrast, at lower frequencies and or larger windows of analysis, there is interference from deeper channel elements, as in the case presented on Figure 3.

The most evident finding is that with the increase in noise content, interpretation becomes more challenging since the amount of noise hinders channel element edge and facies detection. A particular result found is a low coherence value predominance when evaluating the 30% noise case (Figure 10B).

5.5. Pitfalls in attribute interpretation and how to minimize them

The results mentioned above warn of potential pitfalls when interpreting seismic data. For example, not understanding the frequency content and quality of the seismic dataset could result in the inappropriate use of seismic attribute parameters and subsequent misinterpretations. To summarize all these results, we present a list of common pitfalls (Table 3) in attribute interpretation and how the interpreter can attempt to avoid them.

Common misinterpretation	How to address it	Comments
Not inspecting the frequency content and dominant frequency of the data	Inspect the seismic volume and understand dominant frequency and variations with depth	Higher frequency, broader bandwidth data provide higher vertical and lateral resolution
Not understanding the quality of the data and resolution	Calculate the seismic resolution	Imaging of different scales of architecture improves with a higher signal-noise ratio
Using meaningless attributes	Have a clear geological goal and calculate attributes effective for similar targets in literature	Avoid attributes that make pretty pictures but are not directly related to the target objective.
Using default parameters	Select parameters adequate to your study. In windows-based attributes, smaller windows provide less vertical mixing whereas larger windows are less sensitive to noise. Because data quality and resolution change with depth, parameters appropriate for the shallow part may be suboptimum for the deeper part of your survey.	Defaults are provided for the most common cases encountered by the most common user (e.g., oil and gas exploration). If your data are unique in either acquisition or objective, test a wide variety of parameters and choose the ones that best delineate your target.
Interpreting data that has a low S/N ratio, or high noise	Inspect your seismic volume and categorize the noise type and level when possible. Then apply a noise reduction or removal algorithm	Noise can hinder the interpretation of seismic facies and calculating attributes won't help. If data are noisy, we recommend just using amplitude-related attributes.

Table 3. Common pitfalls in seismic interpretation and how to avoid them.

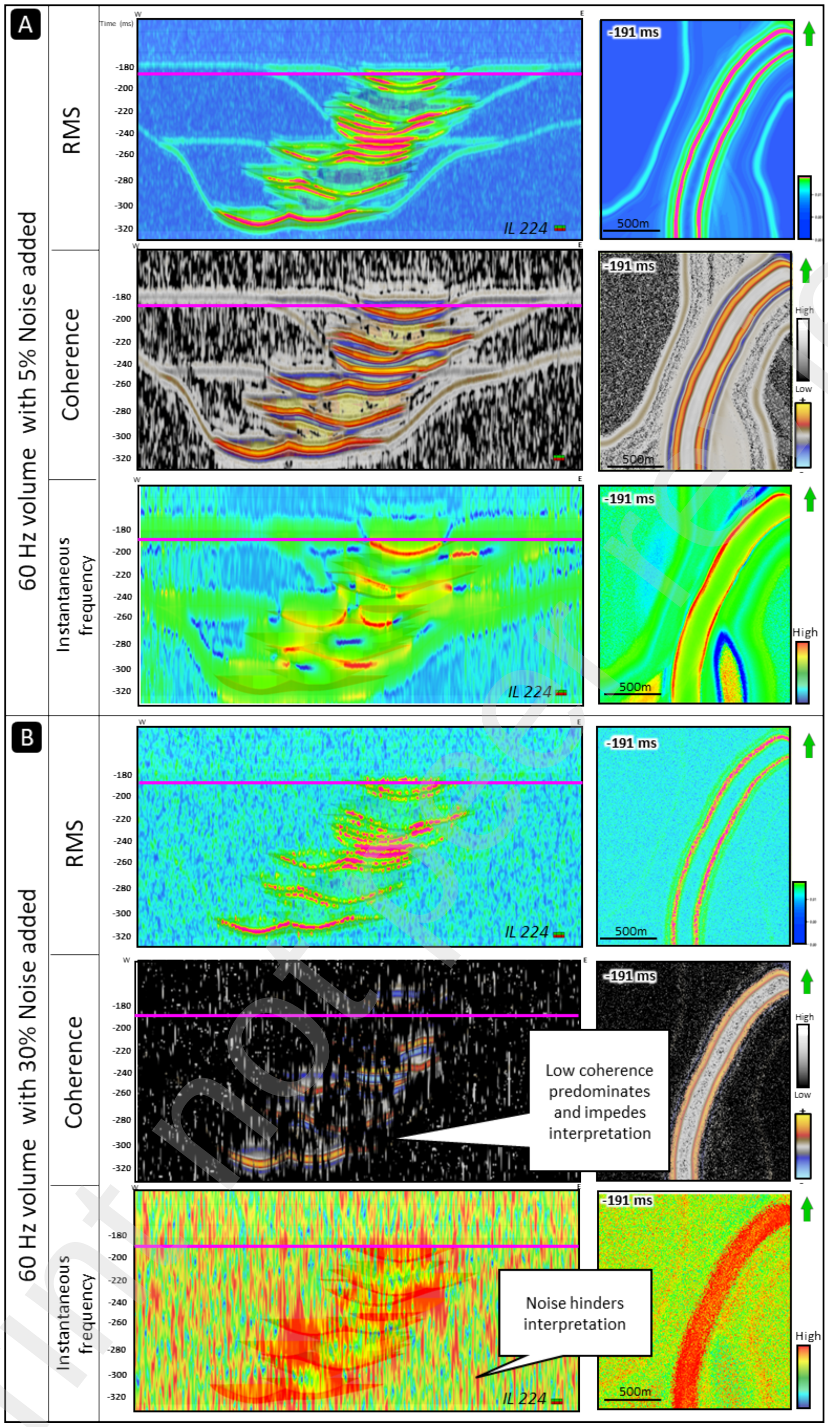

Figure 10. Sensitivity analysis of the effect of random noise in channel architecture interpretation. Results shown refer to the 60 Hz dominant frequency seismic volume (which would be analog to real datasets). (A) 5% band-limited random noise added evaluated in RMS, Coherence, and Instantaneous frequency attributes. Interpretation of prominent features like channel complexes is only possible. (B) 5% band-limited random noise added applied to RMS, coherence, and instantaneous frequency attributes. Notice how the increase in noise is detrimental in the channel architecture interpretation, especially when using coherence. This may be due to the sensitivity that small windows have on high noise content.

6. Discussion

6.1. The importance of mapping channel architectures

Channels systems, whether fluvial or deepwater in origin, exhibit petrophysical characteristics that make them excellent reservoirs for oil, gas, or other resources (Slatt et al., 2009). However, channel system mapping in the subsurface becomes challenging, especially when only seismic data is available.

In seismic reflection data, the amplitude, frequency, and noise content will condition the quality of the seismic image, affecting the interpretation of different architecture and facies embedded in the reflector configuration and overall seismic response. It is, therefore, paramount to understand how size-dependent architecture is displayed and imaged under different conditions and how the application of seismic attributes could help or hinder the interpretation of such architecture.

In this study, we used a unique approach by employing 3D synthetic seismic datasets as a benchmark to perform a sensitivity analysis to understand how different-scales of architecture appear as a function of frequency content, noise level, type of seismic attribute, and parametrization, especially the analysis window selected to calculate attributes.

The analysis of all the scenarios resulted in the following observations: broadband higher frequency data (e.g., 90 and 180 Hz) combined with a short analysis window (e.g., 2 ms, 20 ms) minimized the stratigraphic mixing (Figure 6). In contrast, lower frequency data that were analyzed using a large vertical analysis window (Figure 8) resulted in poor imaging of the channel architecture, vertically mixing stratigraphic architecture at different hierarchical levels. This affects the temporal evaluation of features that show an overlap of individual architecture (i.e., channel elements) in the system in consecutive time slices, or in other words, a vertical offset from the known position (Figure 9) of sedimentary units (also shown by Pemberton et al., 2018).

This observation warns of potential interpretation pitfalls in applying such seismic attributes to actual seismic data. Stratigraphic mixing can hinder the correct temporal and spatial representation of individual channel elements and boundaries of channel complexes, leaving the internal architectures and potential fluid flow barriers imprecisely imaged (Coleman, 2000), hence, incorrectly mapping and estimating the volume of the reservoir units of interest, which could result in important economic loses.

6.2. The effect of frequency content in the imaging of architectural elements

Resolution has always been one of the main concerns for seismic interpreters since important features like small channels, or DHIs/ bright spots can be overlooked in seismic data. Also, hazards and baffles (Cardona, 2020; Meirovitz et al., 2020; Ruetten, 2021), like the MTDs, may not be imaged in the seismic picture analyzed. In this study, MTDs are only five meters thick and usually mantle the base of the channel complexes and complex sets.

To improve the seismic data's resolution, as demonstrated in this study by the enhanced definition of each element in higher frequency datasets, frequency content should be increased. This suggests that ideally, modifying the initial design of the seismic data and obtaining higher frequency data will allow us to get the resolution required to image submarine channel complexity to the detail commonly observed in outcrop (Coleman et al., 2000). This type of data is, however, costly.

Although the cost of high-quality data is currently high, with the advancement in technology, we presume that access to higher-quality data at reduced prices will become available soon. An example of this kind of data is the use of OBN (ocean bottom nodes) – high-resolution 3D seismic acquired with the addition of P-Cable, an offshore seismic data acquisition system that provides highly detailed ultrahigh-resolution images of the seafloor and subsurface geology (McGregor et al., 2022) – and high-resolution (1-6 kHz) chirp data that offer a better image of the stratigraphy and structure of rocks in the shallow subsurface.

It is likely that soon most of the seismic data acquired will be high resolution, without necessarily needing to be high frequency, and that we will find ways to improve our algorithms to treat the noise associated with acquisition and processing or overall improve the data quality from the early stages of seismic acquisition. But, until then, we need to understand the limitations of various kinds of seismic data and become aware of potential pitfalls in interpretation.

6.3. Selecting seismic attributes and parameters that are ideal for mapping channel architecture

In this study, we evaluated the effect of seismic attributes on the channel system architecture interpretation and their true position in the outcrop model. Our first insight is that there is no one-size-fits-all kind of seismic data.

Therefore, we suggest that the first step when interpreting seismic reflection data should be to 1) define the geological goal, 2) become familiar with the acquisition and processing of information, 3) make an initial inspection of the data, 4) determine if there is some noise or artifact that the interpreter needs to correct or be aware of. Finally, 5) select seismic attributes based on established purpose/geological goal.

One of the most critical steps is defining a clear geological goal. The interpreter should reflect on what attribute would better suit their purpose. For example, we would use amplitude-derived or instantaneous attributes in studying bright spots. For channel systems, instantaneous or frequency attributes can help highlight the differences between the channel elements (Fedorova, 2016), whereas geometrical attributes (such as Sobel filter coherence) aid in delineating the external shape of the architecture (La Marca, 2020).

Because there are tens to hundreds of attributes, testing many of them can be time-consuming. Imagine that in this study, with just three attributes shown and the case combinations, we had a total of 90 volumes to evaluate. Therefore, it is recommended to work only with attributes whose principles the interpreter understands or, if using multiple attributes, rely on experimental designs like Box Behnken (Ferreira et al., 2007) that will help to synthesize a large amount of data.

Attribute computation varies from software to software, and some attributes are computed trace by trace, whereas others are sample by sample. Understanding this initially would help in setting the correct parameters in each case. For attributes that are window based, like wavelet or average frequency, and the ones studied here, the variation of the analysis window affects the imaging of architectural elements.

We used instantaneous frequency since it can indicate the edges of thin low-impedance thin features. Additionally, it is an excellent bed thickness indicator, where higher frequencies indicate sharp interfaces or thinly bedded strata and lower frequencies indicate thickly bedded sandstone-rich strata (Subrahmanyam and Rao, 2008). Interestingly, in the study, the true thickness of isolated channel elements (approximately 25m of thick-bedded amalgamated sandstone at the channel element axis) was more interpretable from the dataset of 60 Hz dominant frequency and above and only partially distinguishable in the shallow portion of the 30Hz dataset. This finding was also noted by Nielson (2018) and Langenkamp (2021), although neither study included seismic attribute analysis.

RMS amplitude measures reflectivity within a time window (Meek, 2015). It computes the square root of the sum of squared amplitudes divided by the number of samples within the windows used (Equation 1). Therefore, the number of samples and windows used affects the strength of reflectivity we get with the algorithm used. In contrast, some attributes like Sobel filter coherence do not necessarily improve channel architecture imaging by selecting a minimal analysis window. In this case, since the wavelength increases with increasing velocity, which increases with depth, we agree with Lin et al. (2014) that coherence attributes should use a shorter analysis window in the shallow section and a larger vertical analysis window in the deeper section. Some software has this already integrated as an adaptive window, which we consider to be one route to improve attribute results in the future.

6.4. Impact of noise on the interpretation of channel features

Different types of noise could be found in our seismic data: coherent noise, a series of unwanted signals that appear when the source is applied (Alderton and Elias, 2021), and incoherent noise, which would appear whether we shoot or not. For this sensitivity analysis, we only explored the effect of band-limited random noise, which belongs to the latter category, on imaging the different architecture in a deepwater channel system.

When using instantaneous attributes such as instantaneous frequency, it was noticed that at low noise levels (e.g., 5%), smaller features like MTDs were still visible. However, with the increase in noise, it was extremely difficult to interpret individual geologic features in the seismic volume.

As Herron (2011) stated, the output's quality of interpretability relies on the input's noise content. In fact, a highly noisy dataset will likely contain very little reliable information. Moreover, we noticed that the effect of stratigraphic mixing is emphasized in the coherence attribute, where anomalous low or high values of the attribute were unexpectedly found and that the interpretation of small or large size features in the seismic was very hard to impossible to perform. These findings stress the importance of noise removal using adequate techniques related to the type of noise. This must be done in the early stages of seismic interpretation to avoid misinterpretations (Figure 11).

In terms of the analysis window selected in the presence of noise, using a very large data-analysis window (in three dimensions) will include plentiful data and likely produce output with a marked structural overprint. On the contrary, a window that is too small will barely include data and produce an outcome that is more a manifestation of noise in the data rather than geological content (Herron, 2011).

Our final thoughts are that although studies that use synthetic data and perform sensitivity analyses provide a tool to address misinterpretations encountered in the seismic interpretation of potential reservoirs, especially in the exploration stage, it is necessary to take into account that each seismic dataset and geologic setting are unique to the exploration area and that every aspect should be considered carefully before making impactful decisions.

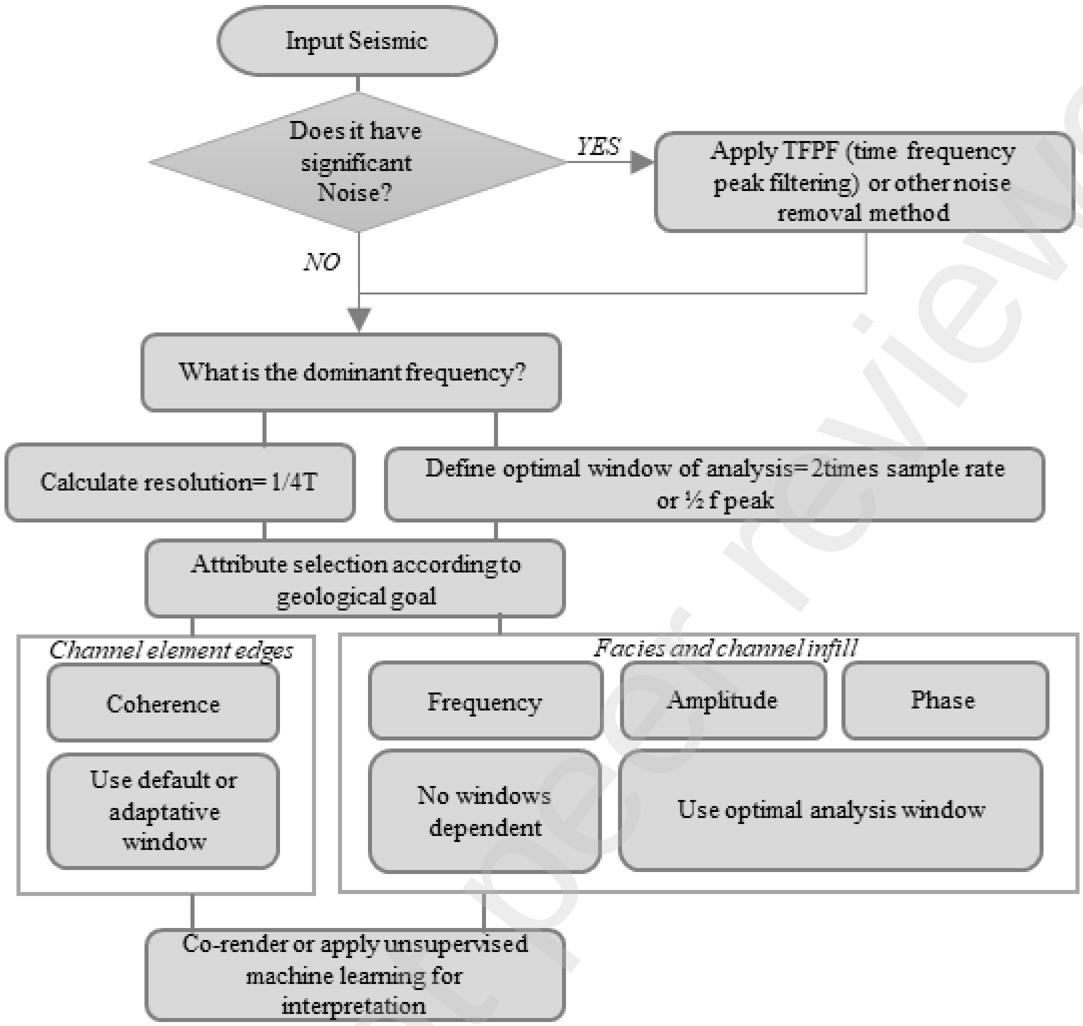

Figure 11. Generalized workflow for a geoscientist to avoid pitfalls in interpretation by getting optimized results according to their dataset.

7. Conclusions

The sensitivity analysis of 3D synthetic seismic volumes derived from a model of an outcropping deepwater slope-system and assigned reservoir properties was performed. The study comprised the combination of four parameters: 1) frequency content, 2) attribute selection, 3) windows of analysis and 4) noise content to identify their effects on the imaging of different scales of deepwater architecture.

The results are summarized in four cases that allow the depiction of common pitfalls in channel interpretation: 1) the effect of the spectral bandwidth on the imaging of the different scales of architectural elements, 2) the seismic attribute sensitivity to the thickness and extent of element and complexes, 3) the effect of the analysis window size on the vertical smearing of channel elements and MTDs, and 4) the effect of noise in the sensitivity analysis.

In this study, we introduced the term "stratigraphic mixing" to define the combined picture resulting from the inability to resolve a single channel element. In this sense, broadband, higher bandwidth (e.g., 90 Hz) data combined with a short analysis window (e.g., 2ms) minimizes stratigraphic mixing. In contrast, lower bandwidth data, in addition to a large analysis window, results in poor imaging of the channel element and channel complexes that exhibit a "composite" appearance, vertically mixing geological features at different stratigraphic levels.

The importance of this analysis resides in that stratigraphic mixing affects the temporal evaluation of features that show an overlap of individual architecture at different scales in the system in consecutive time slices or a vertical offset from the known position of sedimentary units, which may result in important economic losses by misplacing an exploration well (e.g., actual target not in place) or overestimating reserves due to an incorrect NTG estimation and subsequent volumetric calculation (e.g., baffles like MTD are not imaged).

In order to determine the sensitivity of the different architectural elements to seismic attributes, we explored three classes of algorithms: amplitude-based, geometrical, and instantaneous, and showed the results of the most prominent attributes: RMS amplitude, instantaneous frequency, and Sobel filter coherence.

Attributes that are window-dependent, such as RMS amplitude, show an improved imaging of the actual thickness of the channel architecture when calculated using a short analysis window (e.g., 2ms) over a higher frequency dataset (from 30Hz and above). With larger analysis windows and or a small frequency dataset, there is significant vertical stratigraphic mixing. High RMS values and a composite effect were found in stacked channel element configurations indistinctly of the parameters used, which would likely result in an overestimation of NTG.

Conversely, for edge detection attributes like coherence, a small analysis window does not provide a better depiction of channel element/complex/complex set edges. Instead, we observed displacement with respect to the actual position and composite pictures of them, especially in vertical sections, which makes their interpretation cumbersome. Therefore, we suggest using an adaptative window with depth or a default analysis window (half of the peak frequency is a good approximation).

When evaluating the last parameter, which corresponds to the effect of band-limited noise content, it was observed that the mapping of channel elements is hindered by adding noise to the data. When the noise level increases, as expected, the interpretation of features is hindered by the impact of the noise. We suggest applying algorithms that will allow us to eliminate or reduce the noise before calculating any seismic attribute.

Our observations warn of potential interpretation pitfalls in applying default attributes to real seismic data, especially when using geometrical attributes and others that are windows dependent. We offered a simplified workflow for geoscientists to understand and address these concerns depending on their available data.

The importance of using synthetic data to reduce uncertainty is proved. This data allows essaying multiple scenarios to provide tools that serve geoscientists that face different kinds of datasets around the world and help reduce uncertainty by applying best practices in seismic interpretation, especially in channel deposit settings.

Best practices in interpretation should be documented more often to better address uncertainty and optimize reservoir characterization.

Data Availability

Dataset presented at this article can be found at https://data.nzpam.govt.nz/GOLD/system/mainframe.asp, an open-source online data repository hosted at New Zealand and Petroleum Minerals. Synthetic data and model need to be requested to authors.

Acknowledgments

We thank SLB and AASPI (University of Oklahoma) for the software used for attribute and noise computation and visualization; and the Chile Slope Systems Consortium (and sponsors) for providing the synthetic data and 3D model. Thanks to NZPM for providing the Pipeline 3D dataset. Additionally, thanks to the AASPI group at OU and SEG organization for their financial support. Special appreciation to Thang Ha, David Lubo-Robles, Emily Jackson, Teresa Langenkamp, and Diana Salazar for their technical input for this study.

References

Alderton, D., and S. Elias, 2021. Encyclopedia of Geology. Second edition. Elsevier ISBN 978-0-08-102909-1

Barnes, A., 2016. Handbook of Poststack Seismic Attributes: Geophysical References Series, **21**, The Society of Exploration Geophysicists, 254 p

Cardona. S., L. Wood., D. Brandon., Z. J., and Strachan. L, 2020. Characterization of the Rapanui mass-transport deposit and the basal shear zone: Mount Messenger Formation, Taranaki Basin, New Zealand: Sedimentology, **67**, 2111-2148.

Chen, Y., M. Zhang., M. Bai., and W. Chen, 2019. Improving the signal-to-noise ratio of seismological datasets by unsupervised machine learning: Seismological research letters. **90**, 4. Doi: 10.1785/0220190028.

Chopra, S., and K.J. Marfurt, 2020. Adopting multispectral dip component for coherence and curvature computations: The leading edge. **39** (8). 593-596, doi: 10.1190/tle39080593.1.

Chopra S., and K.J. Marfurt, 2007. Seismic attributes for prospect identification and reservoir characterization. Society of Exploration Geophysicists, Tulsa, doi: https://doi.org/10.1190/1.9781560801900.fm.

Coleman Jr., F. C. Sheppard., and T. K. Jones, 2000. Seismic resolution of submarine channel architecture as indicated by outcrop analogs, *in* A. H. Bouma and C. G. Stone., Fine-grained turbidite systems, AAPG Memoir 72/SEPM Special Publication **68**, p. 119–126.

Enwenode, O., 2014. Understanding Noise in Seismic Record: Seismic Data Analysis Techniques in Hydrocarbon Exploration. 63-68. Doi: 10.1016/B978-0-12-420023-4.00004-6.

Fashagba, I., P. Enikanselu., L. Ademola., and M. Olabode, 2020. Seismic reflection pattern and attribute analysis as a tool for defining reservoir architecture in 'Sabalo' field, deepwater Niger Delta: Journal of Petroleum Exploration and Production Technology. Vol **10**. Issue 3. Springer. https://doi.org/10.1007/s13202-019-00807-1

Fedorova, E.V., N.V. Bukhanov., and V.E. Baranov, 2016. Synthetic Seismic Models Construction for Detailed Geological Outcrop. 7th EAGE Saint Petersburg International Conference and Exhibition. DOI: https://doi.org/10.3997/2214-4609.201600270

Ferreira, S.L.C., R.E. Bruns., H.S. Ferreira., G.D. Matos., J.M. David., G.C. Brandao., E.G.P. da Silva., L.A. Portugal., P.S. dos Reis., A.S. Souza., and W.N.L. dos Santos, 2007. Box-Behnken design: an alternative for the optimization of analytical methods: Analytica chimica Acta 597, 179-186.

Fildani, A., S. M. Hubbard., J.A. Covault., K.L. Maier., B.W. Romans., M. Traer., and J.C. Rowland, 2013. Erosion at inception of deep-sea channels: Marine and Petroleum Geology, **41**, pp.48-61.

Fletcher, S., 2013. Stratigraphic characterization of a Cretaceous slope channel complex in the Tres Pasos Formation, Arroyo Picana-Laguna Figueroa outcrop belt, Chilean Patagonia: MS Thesis, University of Calgary.

Herron, D, 2011. First steps in seismic interpretation: Geophysical monograph series, **16**. SEG.

Hossain, S, 2020. Application of Seismic Attribute Analysis in Fluvial Seismic Geomorphology: Journal of Petroleum Exploration and Production Technology **10**, no. 3: 1009–19. https://doi.org/10.1007/s13202-019-00809-z.

Jackson, A., L. Stright., S.M. Hubbard., and B.W. Romans, 2019. Static connectivity of stacked deepwater channel elements constrained by high-resolution digital outcrop models: AAPG Bulletin, **103**(12), 2943–2973, doi: 10.1306/03061917346

Kumar D., and I. Ahmed, 2021. Seismic Noise. *in*: Gupta H.K. Encyclopedia of Solid Earth Geophysics. Encyclopedia of Earth Sciences Series. Springer, Cham. https://doi.org/10.1007/978-3-030-58631-7_146

La Marca, K. and H. Bedle, 2022. Deepwater seismic facies and architectural element interpretation aided with unsupervised machine learning techniques: Taranaki basin, New Zealand. *Marine and Petroleum Geology*, **136**, p.105427.

La Marca, K., 2020. Seismic attribute optimization with unsupervised machine learning techniques for deepwater seismic facies interpretation: Users vs machines: M.S. thesis, The University of Oklahoma

La Marca, K, and H. Bedle, 2022. Deepwater seismic facies and architectural element interpretation aided with unsupervised machine learning techniques. Taranaki basin, New Zealand. 2021: Marine and Petroleum Geology. 105427. https://doi.org/10.1016/j.marpetgeo.2021.105427

Langenkamp, T., L. Stright., H. Bedle., M. Hubbard., and B. Romans, 2020. Quantifying heterogeneity preserved in inverted seismic data: implications for reservoir prediction and geostatistical modeling: presented at the ACE 2020 annual meeting, AAPG.

Langenkamp, T, 2021. Evaluating the impact of deepwater channel architecture on the probability of correct facies classification using 3D synthetic seismic data. Ms. C thesis. Colorado State University.

Lin, T., J. Guo., B. Zhang., K.J. Marfurt., and D. Chang, 2014. Seismic Attributes Estimation Using a Self-Adaptive Window: SEG Technical Program Expanded Abstracts 2014, 1654–58. Denver, Colorado: Society of Exploration Geophysicists. https://doi.org/10.1190/segam2014-1564.1.

Liu, J., and K.J. Marfurt, 2007. Instantaneous spectral attributes to detect channels: GEOPHYSICS. **72**, 2. Doi: 10.1190/1.2428268

Luo, Y., W. G. Higgs, and W. S. Kowalik, 1996. Edge detection and stratigraphic analysis using 3D seismic data: 66th Annual International Meeting, SEG, Expanded Abstracts, 324–327.

Lyu, B., J. Qi, F. Li., Y. Hu, T. Zhao, S. Verma, and K.J. Marfurt, 2020. Multispectral coherence: which decomposition should we use? *Interpretation*. **8**(1), T115- T129, doi: 10.1190/INT-2019-0124.1

Macauley, R. V., and S.M. Hubbard, 2013. Slope channel sedimentary processes and stratigraphic stacking, Cretaceous Tres Pasos Formation slope system, Chilean Patagonia: *Marine and Petroleum Geology*, **41**(1), 146–162, doi: 10.1016/j.marpetgeo.2012.02.004

Marfurt, K. J., R. L. Kirlin, S. H. Farmer, and M. S. Bahorich, 1998. 3D seismic attributes using a running window semblance-based algorithm: *Geophysics*, **63**, 1150–1165, doi: 10.1190/1.1444415

McGregor. L., L. Scott., R. Cooper., and J. Nichols, 2022. Ultra-High resolution seismic: applications of P-Cable in the energy transition: First Break, **40**, 67-70.

McHargue, T., Pyrcz, M. J., Sullivan, M., Clark, J. D., Fildani, A., Levy, M., … Covault, J. A, 2011. Event-based modeling of turbidite channel fill, channel stacking pattern, and net sand volume. *Outcrops Revitalized: Tools, techniques and applications*, **10**, 163-173

Meek. T, 2015. Applications of 3D seismic attribute analysis workflows: a study from Ness County, Kansas, USA. Ms. C. thesis, Kansas State University.

Meirovitz, C. D., L. Stright., S.M. Hubbard., and B.W. Romans, 2020. The Influence of Inter- and Intra-channel Architecture on Deep-water Turbidite Reservoir Performance: *Petroleum Geoscience*, **27**, doi: 10.1144/petgeo2020-005 .

Nielson, A., 2018. Using RMS amplitudes from forward seismic-reflectivity modeling of channelized deepwater slope deposits to inform stratigraphic interpretation and sub-seismic scale architecture, Tres Pasos Formation, Magallanes Basin, Patagonia, Chile: MS Thesis, Colorado State University.

Pemberton, E., L. Stright., S. Fletcher., and S. Hubbard, 2018. The influence of stratigraphic architecture on seismic response: reflectivity modeling of outcropping deepwater channel units: Interpretation, **6** (3), T783–T808. doi: 10.1190/INT-2017-0170.1

Pickering, K.T., Corregidor, J., Clark, J.D., 2015. Architecture and stacking patterns of lower-slope and proximal basin-floor channelized submarine fans, Middle Eocene Ainsa System, Spanish Pyrenees: an integrated outcrop-subsurface study. Earth-sci. Rev. 144, 4-81.

Posamentier, H.W., and V. Kolla, 2003. Seismic geomorphology and stratigraphy of depositional elements in deepwater settings: Journal of Sedimentary Research **7**3, 367-388.

Prather, B.E., 2003. Controls on reservoir distribution, architecture, and stratigraphic trapping in slope settings. Marine and Petroleum Geology 20, 529-545.

Ruetten, A., 2021. Evaluating the impact of hierarchical deepwater slope channel architecture on fluid flow behavior, Cretaceous Tres Pasos Formation, Chile MS Thesis, Colorado State University.

Slatt, R., E. Eslinger., V. Dyke., and K. Staffan, 2009. Acoustic and petrophysical properties of a clastic deepwater depositional system from lithofacies to architectural elements' scales: GEOPHYSICS, **74**. 2. Doi: 10.1190/1.3073760.

Southern, S.J., Stright, L., Jobe, Z.R., Romans, B., and Hubbard, S., 2017. The stratigraphic expression of slope channel evolution: insights from qualitative and quantitative assessment of channel fills from the Cretaceous Tres Pasos Formation, southern Chile: AAPG Annual Convention, Houston, TX, April 3-5, 2017.

Stright, L., Stewart, J., Campion, K. and Graham, S., 2014. Geologic and seismic modeling of a coarse-grained deepwater channel reservoir analog (Black's Beach, La Jolla, California) Seismic Modeling of a Deep-Water Reservoir Outcrop Analog, California: AAPG bulletin, **98**(4), pp.695-728.

Subrahmanyam, P., and P.H. Rao, 2008. Seismic attributes- a review: 7th. International conference and exposition on petroleum geophysics.

Schwab, A. M., B.T. Cronin., and H. Ferreira, 2007. Seismic expression of channel outcrops: Offset stacked versus amalgamated channel systems: Marine and Petroleum Geology. **24**, 6-9, 504-514. Doi: 10.1016/j.marpetgeo.2006.10.009.

Tanimoto, T., K. Heki., and J. Artru-Lambin, 2015. Interaction of Solid Earth, Atmosphere, and Ionosphere. Treatise on Geophysics: Second Edition. **4**. 421-443. Doi: 10.1016/B978-0-444-53802-4.00083-X

LIST OF FIGURES

Figure 1: Stratigraphic hierarchy: from a single element to complex sets. A vertical slice within the Pipeline 3D dataset offshore New Zealand shows the seismic appearance of different architectural hierarchies in deepwater channels, with corresponding cartoons below. The smallest architecture (4th ^{to} 5th order) is the channel element (box 1 in green). The second hierarchy (6th order) occurs when the channel elements stack together, forming a channel complex (box 2 in blue). The higher-order hierarchy (7th order and higher) occurs with the amalgamation of channel complexes, developing a channel complex set (box 3 in magenta). The color legend indicates the distinct facies that commonly occur within each element of each architecture. Measuring the sizes of each architectural element indicated on the right as well as their hierarchy, provides key insight into the underlying depositional processes as well as a prediction of the more common lithologies. Hierarchies mentioned follow Pickering and Cantalejo (2015) classification.

Figure 2. A visual guide showing the steps to convert outcrop measurements to a synthetic model. (A) Location and exposure of the outcropping deepwater channels at Laguna Figueroa. Paleoflow is from North to South (obliquely and to the right into the outcrop at this location) (B) Conceptual diagram of the Upper and Lower Figueroa outcrops showing channel elements, complexes and complex sets. The red line indicates the outcrop profile. Left of the line is into the outcrop face, and the right has been eroded away. (C) geocellular model using the constraints from (B) augmented by facies and corresponding rock properties, including acoustic impedances from Shallow Offshore West African modeled rock properties (Stright et al., 2014). (D) The Ormsby wavelet and a representative vertical slice through the 3D synthetic seismic data volume generated from the model shown in (C). Courtesy of Teresa Langenkamp and Lisa Stright.

Figure 3. Explanation of stratigraphic event mixing or vertical smearing of stratigraphic features. (A) Vertical resolution of channel elements related to different peak frequencies (modified after Nielson, 2011). (B) Vertical slice through the 3D Pipeline 3D offshore New Zealand seismic survey showing a channel complex and a Horizon used for interpretation at different stratigraphic levels indicated by yellow arrows. The dominant frequency at this level is 40 Hz giving a dominant period of 25 ms. (C) Stratal slices at approximately 25 ms intervals through the coherence volume computed using a ±20 ms analysis window show "stratigraphic" mixing by the seismic wavelet. Note that the relatively straight channel form at 2050 ms can be seen at 2080 ms and other

stratigraphic levels (1,2,3 from deeper to shallower) where other channel forms (green arrow) appear causing interference. The cause of this mixing could be 1) mixing of reflectivity by the 25ms dominant period seismic wavelet, 2) mixing of discontinuities through the 40 ms coherence computation, 3) shifting of the basal channel element thalweg due to compensational style as you move up or 4) differential compaction over deeper discontinuities between the floodplain and the channel element fill.

Figure 4. Workflow of the study. Four different parameters were evaluated in the sensitivity analysis: 1) the effect of frequency content, 2) the impact on the choice of the seismic attribute, 3) the analysis window effect, and 4) the sensitivity to band-limited random noise addition. The best cases were selected to be shown in each case, and analysis was performed by comparing them with the original 3D geological model derived from the Laguna Figueroa Deepwater outcrop. This resulted in 4 cases for analysis, ultimately leading to a workflow and documentation of best practices in channel architecture interpretation.

Figure 5. A representative analysis window used in attribute calculations. Signals are sampled at discrete points, not continuous recordings. Therefore, each seismic trace will contain as many samples as the sample rate allows. For the example shown, if we consider the dominant period (distance between two peaks), our analysis window will contain 20 samples, equivalent to ~ 20 msec. Other examples of analysis windows are depicted, including the smallest possible equivalent to the sample increment, in this case, 1 msec.

Figure 6. A representative vertical slice (224) and time slices at t=-191ms) through the (A) 3D model that shows (B) 15 Hz data, (C) 60 Hz data, (D) 90 Hz data, and (E) 180 Hz data. Notice the improvement in the channel architecture's detail with the increase in the dominant frequency and corresponding spectral bandwidth, being able to interpret complexes from figure B on.

Figure 7. Results on the attribute sensitivity analysis to thickness and extent of architectural elements using a default analysis window. We present results on the 30 Hz dataset, analogous to vintage seismic data (to the left), and the 60Hz dataset, representing modern seismic data (to the right). Each attribute is presented for both frequencies in a representative inline (224) and time slices (-280 ms and –191ms) as follows: (A) RMS (Root Mean Square) amplitude for 30 Hz (B) coherence (Sobel filter) for 30Hz, (C) Instantaneous frequency for 30 Hz, (D) RMS amplitude for 60 Hz (E) coherence (Sobel filter) for 60Hz, (F) Instantaneous frequency for 60 Hz.

Figure 8. RMS amplitude sensitivity analysis to evaluate the effect of the window size *W* on the vertical smearing of the different channel elements in the model. (A) 15 Hz with *W*=2ms (B)50 Hz with *W*=50ms (C) 30Hz with *W*=2ms (D) 50 Hz with *W*=50ms (E) 180 Hz with *W*=2 ms (F) 180 Hz with *W*=50 ms. High-frequency data with a small analysis window provides the most suitable representation of the true model. In RMS amplitude, the most accurate facies depiction is given by high frequencies and small window combination, imaging channel element base, and inner and outer levee facies.

Figure 9. Sobel filter coherence attribute sensitivity analysis to evaluate the effect of the window size *W* on the vertical smearing and displacement of the different architectural elements in the model. (A) 15 Hz with *W*=2ms (B)30 Hz with *W*=2ms (C) 60Hz with *W*=2ms (D) 60 Hz with *W*=50ms. Notice how at a higher dominant frequency (60Hz) and smaller window of analysis, there is better detection of the channel element edges and channel element fill. In contrast, at lower frequencies and or larger windows of analysis, there is interference from deeper channel elements, as in the case presented on Figure 3.

Figure 10. Sensitivity analysis of the effect of random noise in channel architecture interpretation. Results shown refer to the 60 Hz dominant frequency seismic volume (which would be analog to real datasets). (A) 5% band-limited random noise added evaluated in RMS, Coherence, and Instantaneous frequency attributes. Interpretation of prominent features like channel complexes is only possible. (B) 5% band-limited random noise added applied to RMS, coherence, and instantaneous frequency attributes. Notice how the increase in noise is detrimental in the channel architecture interpretation, especially when using coherence. This may be due to the sensitivity that small windows have on high noise content.

Figure 11. Generalized workflow for a geoscientist to avoid pitfalls in interpretation by getting optimized results according to their dataset.

LIST OF TABLES

Table 1. Tuning thicknesses for shallow and deep elements in each synthetic seismic volume. Modified from Langenkamp (2021).

Table 2. Selected seismic attributes to perform the sensitivity analysis showing a representative image, feature measurement, and use in channel element interpretation.

Table 3. Common pitfalls in seismic interpretation and how to avoid them.

APPENDIX

A- Specs for each synthetic volume

Dominant Frequency (Hz)	Length (ms)	Sample rate (ms)	Low-cut Frequency (Hz)	Low-Pass Frequency (Hz)	High-Pass Frequency (Hz)	High-cut Frequency (Hz)
15	200	1	1	3	23	35
30	200	1	2	6	45	70
60	100	1	4	12	90	140
90	100	1	6	18	135	210
180	26	1	10	30	225	350